Application of phase shift focus monitor in EUVL process control

Lei Sun*[a], Sudhar Raghunathan[a], Vibhu Jindal[b], Eric Gullikson[c], Pawitter Mangat[a], Iacopo Mochi[c], Kenneth A. Goldberg[c], Markus P. Benk[c], Oleg Kritsun[d], Tom Wallow[d], Deniz Civay[a] and Obert Wood[a]

[a]GLOBALFOUNDRIES, 257 Fuller Rd, Suite 3100, Albany, NY 12203 USA;
[b]SEMATECH, 257 Fuller Rd, Suite 2200, Albany, NY 12203 USA;
[c]Lawrence Berkeley National Laboratory, 1 Cyclotron Road, Berkeley, CA 94720 USA;
[d]GLOBALFOUNDRIES, 1050 Arques Ave., Sunnyvale, CA 95085 USA.

ABSTRACT

Both 90.9º and 180º phase shifts have been achieved using a new Phase Shift Mask (PSM) structure. This PSM is intended for use as a focus monitor. Both the EUV images of the focus monitor patterns on the new EUV PSM test mask, obtained from the SEMATECH/Berkeley Actinic Inspection Microscope (AIT), and the SEMATECH EUV Micro Exposure Tool (MET), shows that an alternating PSM EUV mask can be effectively used for EUVL focus monitoring.

Keywords: phase shift mask, Extreme ultraviolet lithography, EUV, focus monitor, lithography

1. INTRODUCTION

Focus control is becoming more and more important in lithography as Depth of Focus (DOF) shrinks. DOF is inversely proportional to the square of Numerical Aperture (NA). Since NA must be increased continually to improve the lithography resolution, DOF has to shrink accordingly. Even though modern lithographic scanners have internal focus sensors, focus error can still arise from scanner assembly problems, maintenance issues, geographical and environment differences. Therefore, focus measurement methods providing an independent test of the on-board metrology are preferred. Many different methods have been proposed to measure focus error on the aerial image in a scanner, such as, measuring the latent image contrast as a function of focus offset[1], visual observation of dot arrays through focus[2], Bossung plot generated from a Focus-Exposure-Matrix (FEM)[3], and Phase Shift Focus Monitor (PSFM) based on Alternating Phase Shift Mask (Alt. PSM)[4].

The PSFM is one of the most popular focus measurement methods due to its simplicity and resist-based nature. It was first suggested by T. Brunner[4] in 1994 and provides a very sensitive way to determine focus errors from changes in the position of target patterns in resist. Alt. PSM is now widely used for focus and aberration monitoring in deep ultraviolet lithography[5-7]. With Extreme Ultraviolet Lithography (EUVL) inserting into semiconductor manufacture soon[8], EUV Alt. PSM is needed.

M. Sugawara[9] proposed one Alt. PSM with absorber and Molybdenum (Mo) deposited above different sections of Multilayer (ML) on the mask in 2003. The light reflected from absorber and Mo areas have 180º phase shift. However, this method made the fabrication complex and reduced the mask reflectivity. P. Yan[10,11] proposed one Alt. PSM based on the glass substrate etching. ML is deposited on etched substrate and different etching thickness contributes to the 180º phase shift. However, the ML lateral transition width between different etching areas is larger than 60 nm on mask scale and limits its applications at small technology nodes. La Fontaine[12] proposed etched ML Alt. PSM in 2006, but the etching thickness control and time degradation proved to be problematic. Etching Stop Layer (ESL) was proposed to improve the etched ML Alt. PSM idea[13,14]. All of these previously proposed Alt. PSMs focused on Alt. PSM fabrication and resolution enhancement, but never on focus monitoring.

---

*Email: lei.sun@globalfoundries.com, Phone: 1-518-292-7165

In this paper, we will discuss the development of a novel Alt. EUV PSM that can be used to monitor focus characteristics of a EUV scanner. The measured phase shift angle was 90.9º and is close to the angle (90º) at which a PSFM has its maximum sensitivity. Both the EUV images of the focus monitor patterns on the new EUV Alt. PSM test mask, obtained from the SEMATECH/Berkeley Actinic Inspection Microscope (AIT), and the SEMATECH EUV Micro Exposure Tool (MET) in Albany, shows that focus monitor patterns shift with focus. The same Alt. PSM with 180º phase shift can also be used for aberration monitor, and will be addressed in separate paper[15].

2. ALT. EUV PSM SIMULATION AND PHASE SHIFT CALIBRATION

2.1 Simulation

A new Alt. EUV PSM design different from all the above mentioned EUV PSMs is shown in Fig. 1. A few top layers are coated above the ML of a conventional EUV mask. These top layers are removed selectively after etch. The reflectivity and phase of the reflected light on the un-etched and etched areas are R_1, φ_1, R_2, φ_2, respectively. With well designed top layers, it is possible to have a phase shift, $\varphi_1 - \varphi_2 = 90º$ or 180º, and a balanced reflectivity, $R_1 = R_2$.
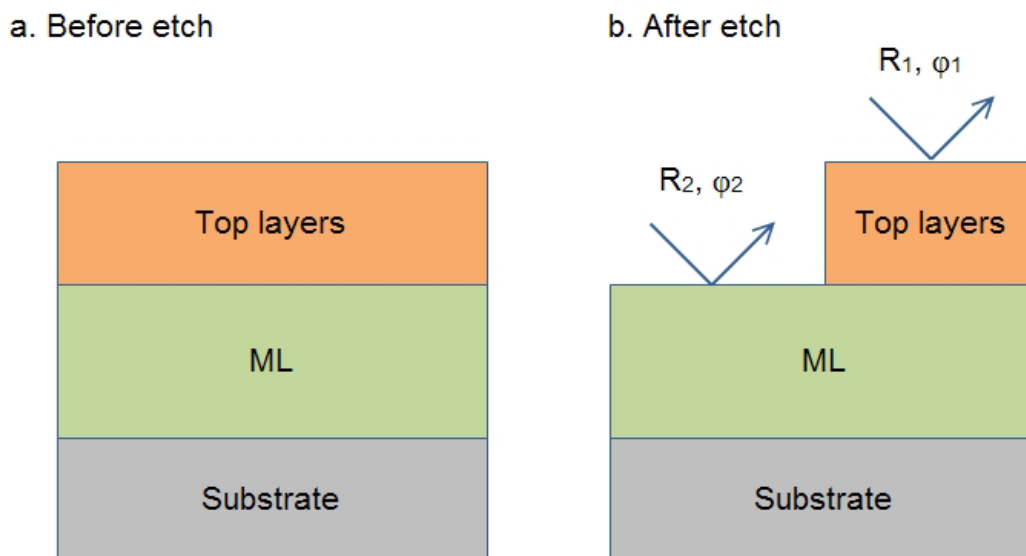

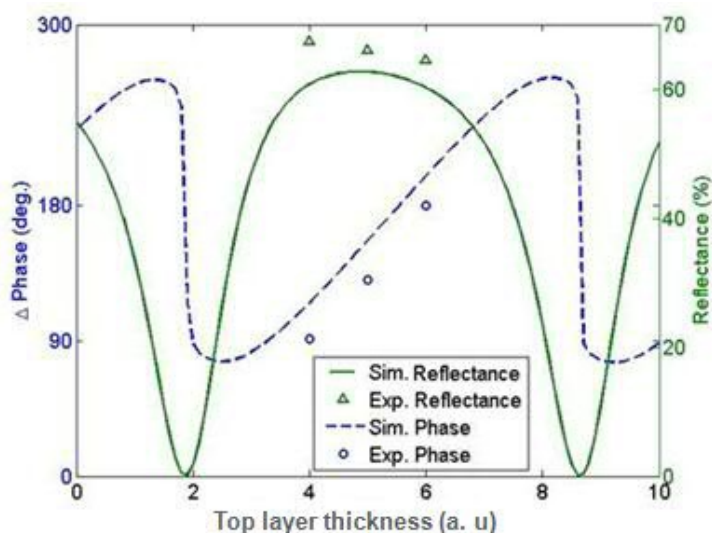Fig. 1. Alt. PSM design, (a) before etch and (b) after etch.

Fig. 2. The experimental and simulated reflectivity on un-etched region and the phase shift of the Alt. PSM.

The simulation of the Alt. EUV PSM is carried out with PANORAMIC software. All the optical constants are from the database of the Center for X-Ray Optics (CXRO), Lawrence Berkeley National Laboratory (LBNL). Fig. 2 shows the experimental and simulated phase shift and R_1 as a function of the top layer thickness. Phase shift changes from 90º to 180º when the top layer thickness changes, while reflection on the un-etched area is almost at a maximum. Experimental data shown in Fig. 1 will be discussed in detail in Section 2.2.

Three quartz substrates for the Alt. EUV PSM test mask were coated with Mo/Si ML at the SEMATECH Mask Development Center in Albany. The blanks were patterned and etched at the Advanced Mask Technology Center (AMTC) in Dresden, Germany.

2.2 Phase shift calibration

Some patterns on the three test masks are shown in Fig. 3(a). The edge of the mask is left un-etched. The blue color area is etched. The two orange color areas are 1D 1:1 alternating phase shift gratings with 2-μm pitch. Other patterns are not shown for simplicity. The mask reflectivity and grating diffraction data were measured with EUV Reflectometry Beamline 6.3.2 at the Advanced Light Source in Berkeley. Wavelength is 13.5 nm in the experiment. The experimental specular reflectivities of the test masks with different top layer thickness are shown in Fig. 3(b), 3(c) and 3(d), respectively. The scan direction, x, used for the measurements is shown in Fig. 3(a).

The measurements show that the reflectivity on the etched and un-etched region are not perfectly balanced. The reflectivity on the etched region for all the test masks is approximately 57%. The reflectivity is a little smaller than the normal ML reflectivity possibly due to etching roughness. It can be increased by optimizing etching technique or increase the number of ML pairs. The reflectivity on the un-etched areas for all the test masks are shown in Fig. 2. They ranged from 67.4% to 64.5%. The difference between the simulation and experiment is due to the interlayer diffusion and optical constants difference. The specular reflection on the grating area is decreased from Fig. 3(b) to 3(d), which is the result of destructive interference for different phase shift.

The experimental diffraction data from the 2-μm grating is plotted as a function of diffraction angle for the 3 test masks in Fig. 4. Zero degree corresponds to the specular reflection direction. The diffraction angle, θ, between each diffraction order is 0.39º derived from the grating equation, $\sin(\theta) = \lambda / pitch$. Diffraction orders from -3 to +3 have been illustrated in Fig. 4(a). Fig. 4 (b) and (c) have similar diffraction order positions. The two peaks near the 0 diffraction order in Fig. 4 (a) and (b) are system errors induced by interference.

The theoretical diffraction distribution of a 1D 1:1 grating can be derived from the Fourier optics[16]. Eqs. 1-3 shows the intensity ratios between diffraction order, 0, 1, 2 and 3, respectively.

$$\frac{I(n=0)}{I(n=1)} = \frac{\pi^2}{4} \cdot \frac{(r_1^2 + r_2^2 + 2r_1r_2\cos\varphi)}{(r_1^2 + r_2^2 - 2r_1r_2\cos\varphi)} \tag{1}$$

$$I(n=2) = 0 \tag{2}$$

$$\frac{I(n=3)}{I(n=1)} = \frac{1}{9} \tag{3}$$

where n=0, 1, 2, 3 are the diffraction orders. r_1 and r_2 are the reflection coefficients from the un-etched and etched areas, respectively. φ is the phase shift between two areas. Since the 3rd order intensities in Fig. 4 are close to noise level, only the ratio between 0 and 1st order are considered during phase shift calibration. The thin mask approximation simulation from PROLITH is also used to verify the phase shift result besides the theoretical and experimental data. The intensity ratio between 0 and 1st orders and the calibrated phase shift for three test masks have been shown in Table 1. 90.9º and 130.3º phase shifts have been achieved for first and second test masks, respectively. Since the 0 order intensity for the third test mask is buried in the noise, the noise level is used to estimate the experimental ratio. The theory and the simulation ratio shows that the phase shift is close to 180º, and the 2.3º is the error induced by the noise. The experimental and simulated phase shift in Fig. 2 has the same trend. The difference is induced by interlayer diffusion and optical constants difference.
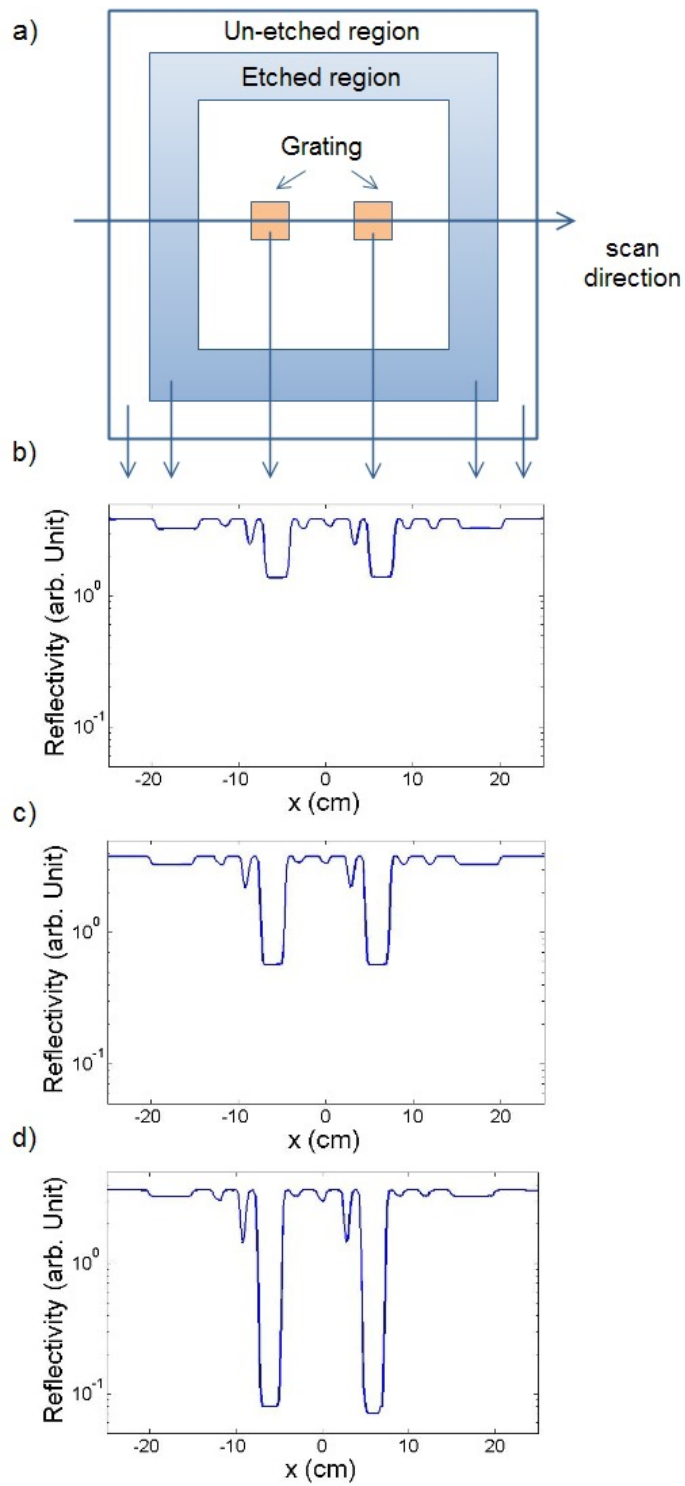
Fig. 3. The mask layout (a) and the reflectivity measurements of the 3 Alt. PSM test masks (b-d).
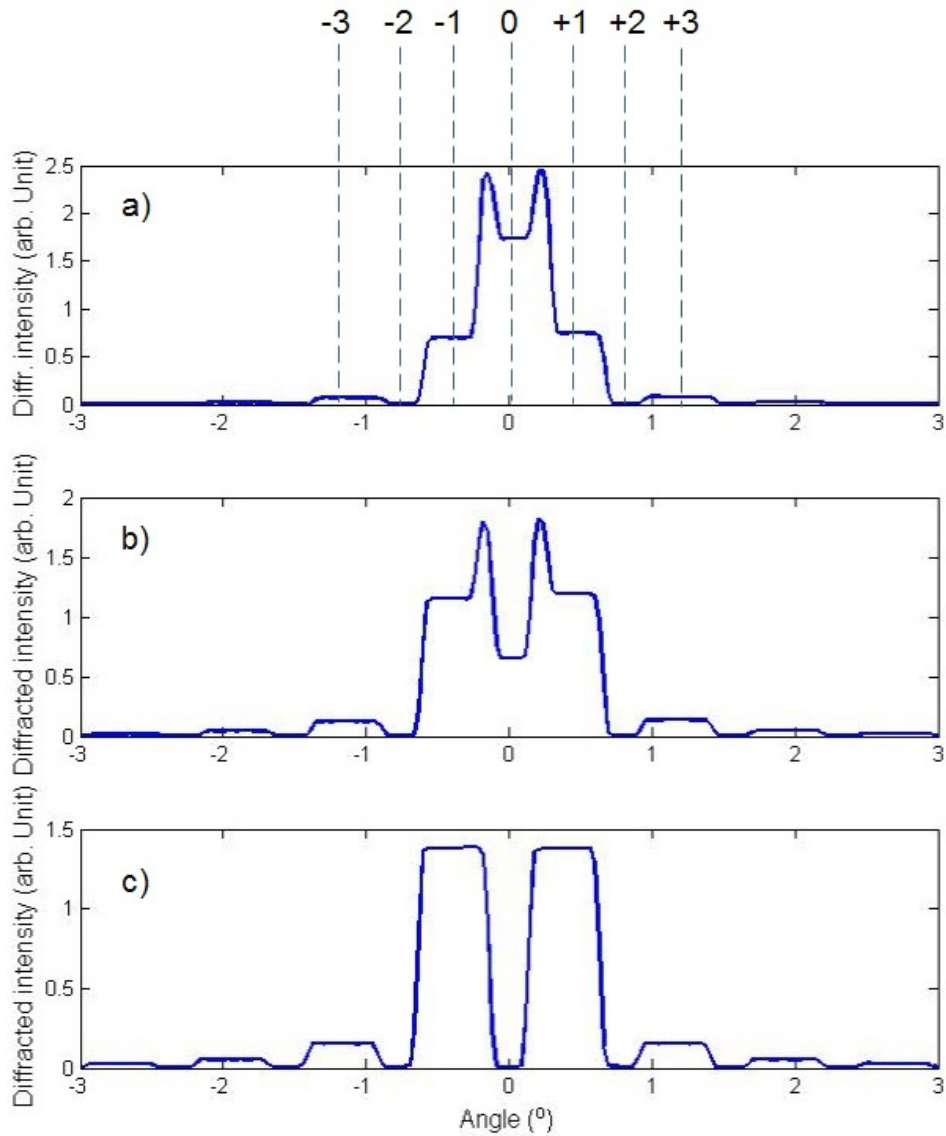
Fig. 4. The experimental 2-μm grating diffraction data from the 3 test masks.

Table 1.Intensity ratio and the calibrated phase shift for three test masks.

Mask	angle (⁰)	Intensity ratio between 0 and 1st order		
		experiment	theory	simulation
1	90.9	2.395	2.395	2.39
2	130.3	0.534	0.534	0.532
3	180.0±2.3	0.0028	0.0018	0.0018

3. APPLICATION OF ALT. PSM IN FOCUS MONITORING

3.1 AIT image

One of the focus monitor patterns on the new Alt. EUV PSM test mask is shown in Fig. 5(a). It consists of two rows of square contact holes. One row consists of phase shifted squares embedded in a phase un-shifted area. Another row consists of phase un-shifted squares embedded in a phase-shifted area. Considering a pair of holes with the same dimension in two rows, their aerial image should also have the same dimension at best focus. If the focus shifts, the dimension of the two contact holes will change in opposite directions due to the phase shift[4, 17, 18]. Therefore, the best focus can be determined when these two contact holes have the same dimension in aerial image.

A EUV image this pattern was obtained from the SEMATECH/Berkeley Actinic Inspection Microscope (AIT), which is shown in Fig. 5(b). The image shows two rows of square contact holes, with un-shifted and 90.9º shifted phases, surrounded by phase shifted and un-shifted regions, respectively. Fig. 5(c) shows a series of two-contact-holes boxes in the orange circle on the Fig. 5(b) when it is scanned through focus. The converted focus step size is 31.25 nm on a 4X scanner system. Since there is no absolute focus position sensor in AIT, there is no straightforward way to determine best focus. A commonly used method to determine best focus is to visually inspect the images. The image with minimum speckle Root Mean Square (RMS) intensity corresponds to the best focus, because it has the best printability. As shown in Fig. 5(c), the 3rd image is determined to be at best focus with this method and focus at other images can be derived from the known focus step.

Critical Dimension (CD) measurement data collected from the actinic images and plotted in Fig. 5(d) shows that the sizes of the contact holes decrease and increase as a function of focus. The crossover of the two set of data corresponds to the position of best focus, which is exactly in agreement with that determined by the visual inspection method.

3.2 MET image

Fig. 6(a) shows the design of a three-bar mask pattern, in which the three bars have been shifted in phase by 90º with respect to the surrounding area on the mask. The distance between the bar edges changes as a function the focus[4, 17, 18]. This pattern was imaged in 50-nm thickness SEVR139 resist using the SEMATECH EUV Micro Exposure Tool (MET) in Albany. One EUV resist image is shown in Fig. 6(b). Fig. 6(c) shows the AIT image of the three bar pattern. The plot of the measurement data shown in Fig. 6(d) shows the distance between the middle bar edges moves smoothly as the focus is changed, which makes this three-bar pattern a good candidate for focus uniformity measurements across the slit of the EUV imaging system or across an entire exposed silicon wafer. Similar to the AIT, the EUV MET does not have an absolute focus sensor. The focus shown in Fig. 6(d) is an estimate.
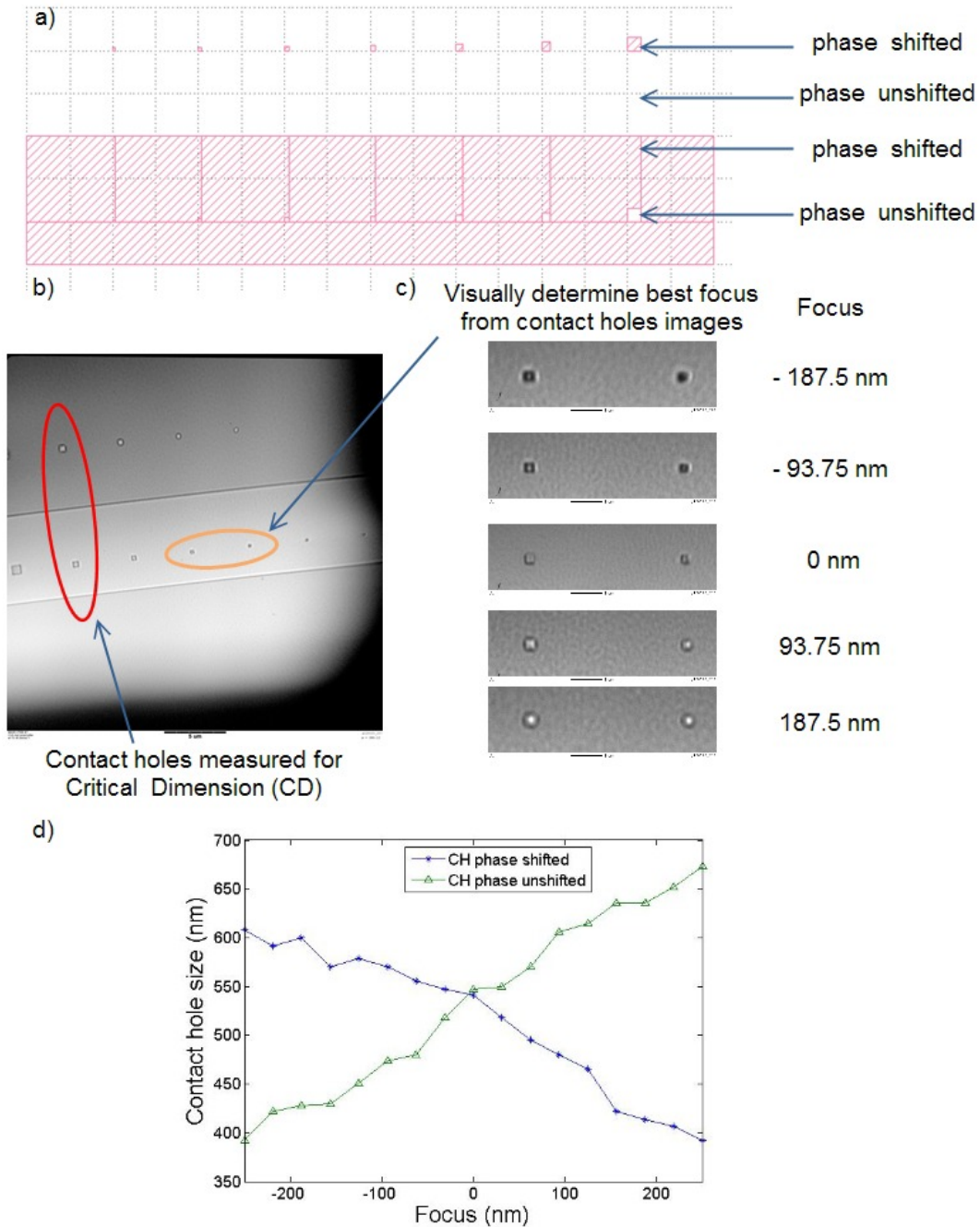
Fig. 5. Figure (a) shows a design of two contact holes boxes which located in phase shifted and un-shifted fields, respectively. Figure (b) shows one actinic image of the two contact holes boxes. Figure (c) shows a series of two-contact-holes boxes in the middle of the figure (b) as a function of focus. The image with minimum speckle Root Mean Square (RMS) intensity corresponds to best focus.   Figure (d) shows that the sizes of the two contact holes in the red circle on the figure (b) decrease and increase, respectively, as a function of the focus. The crossover of the two set of data corresponds to the position of best focus.
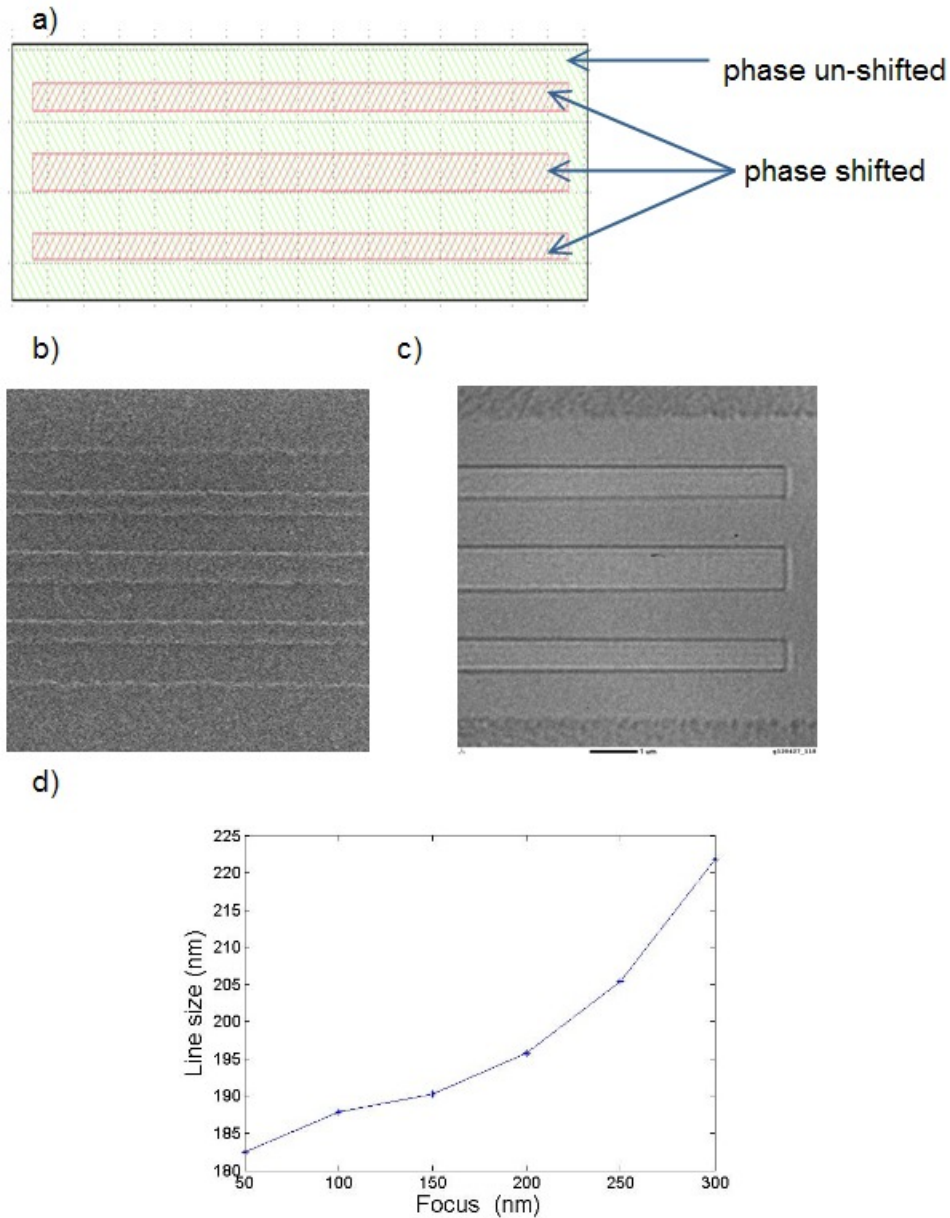
Fig. 6. Figure (a) shows the three-bar pattern design. The three bars have 90º phase shift compared with the surrounding area. Figure (b) and (c) show the MET and AIT images of the three bar pattern, respectively. Figure (d) shows that the distance between middle bar edges moves smoothly as the focus changes.

3.3 Concentric boxes

Another popular focus monitor pattern is the concentric box design shown in Figs. 7 and 8[6, 17]. Fig. 7(a) shows the original concentric box configuration where two boxes made of absorber lines are placed concentrically. The shadow and white color in Fig. 7(a) represents 90º and 0º phase shifts, respectively. Since the inner and outer boxes have opposite tones, they will move in opposite directions when there is defocus. This different direction movement can induce overlay errors, which is shown in Fig. 7(b). Therefore, the defocus can be monitored by overlay errors.

Since CD measurement is used in other focus monitor methods, the focus measurement result is inevitably affected by dose variations. However, this dose variation factor is removed in the concentric box method because the overlay error is only related to the defocus.

In 2002, an improved version of the concentric boxes method was proposed[6, 7]. The single absorber line was replaced by phase shift gratings which are shown in Fig. 8. The phase shift gratings consisting of the inner and outer boxes have reversed tone, respectively. The improved design has better sensitivity than the original design.

Fig. 9 shows the simulated overlay error as a function of defocus for different absorber CD at same 1000 nm pitch. The one-dimensional vertical phase shift grating used in the simulation has same structure as shown in Fig. 8(b). The absorber CD ranges from 60 to 140 nm with 20 nm step. The pitch ranges from 800 to 1400 nm with 100 nm step. The 13.5 nm wavelength, 0.8 partial coherence and 0.25 NA are used in the thick mask PANORAMIC simulation. Fig. 10 shows the total overlay error from +/- 100 nm defocus for various absorber CD and grating pitches. The sensitivity does not depend on pitch but on absorber CD. Smallest line CD has the largest sensitivity, which is around 14.3 nm defocus per 1 nm overlay error.
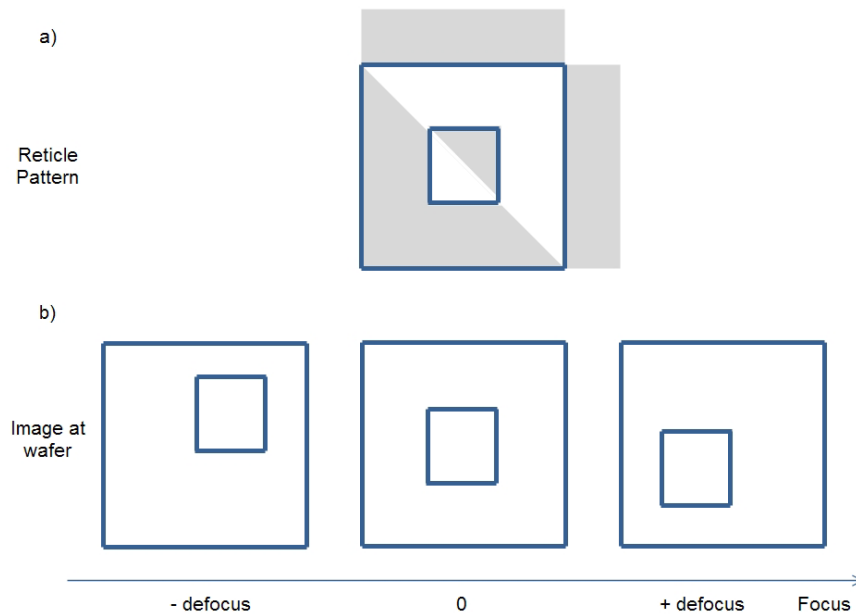

Fig. 7. Figure (a) shows the concentric box design, where shadow and white color represent 90º and 0º phase shift, respectively. Figure (b) shows the overlay errors of the concentric boxes for different defocus.
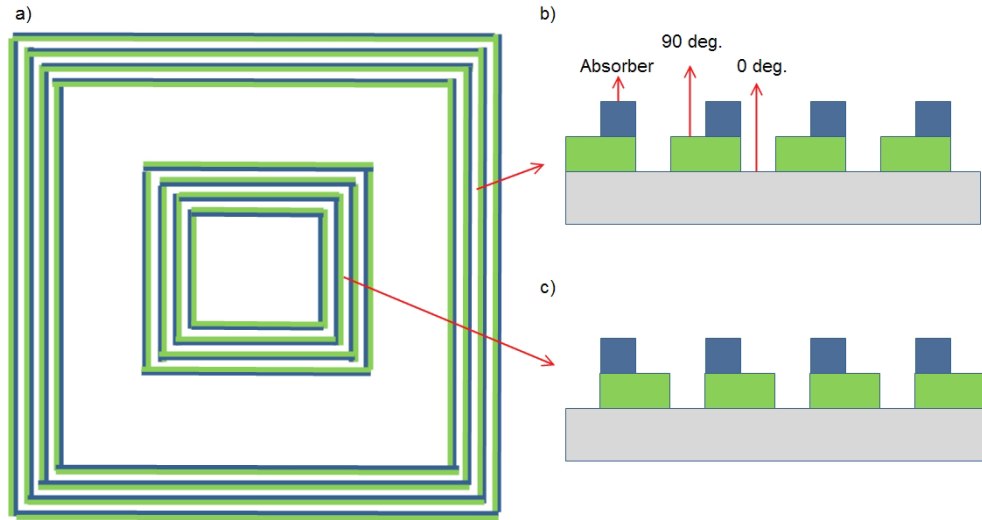
Fig. 8. Concentric boxes design based on phase shift gratings. The gratings on inner and outer boxes have reverse tone, respectively.
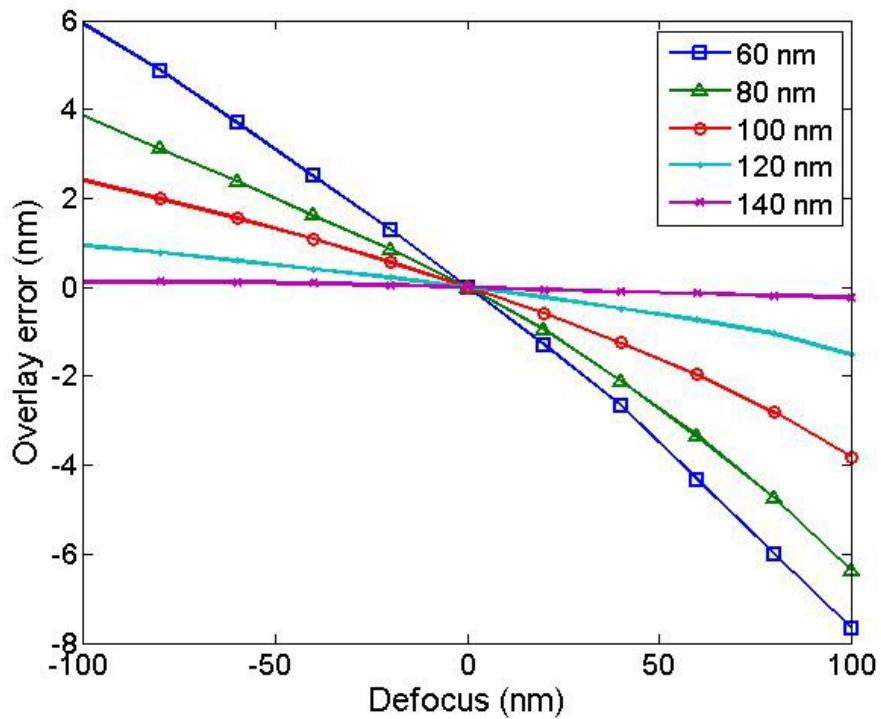

Fig. 9. Simulated overlay error as a function of defocus for different absorber CD at the same 1000 nm grating pitch.
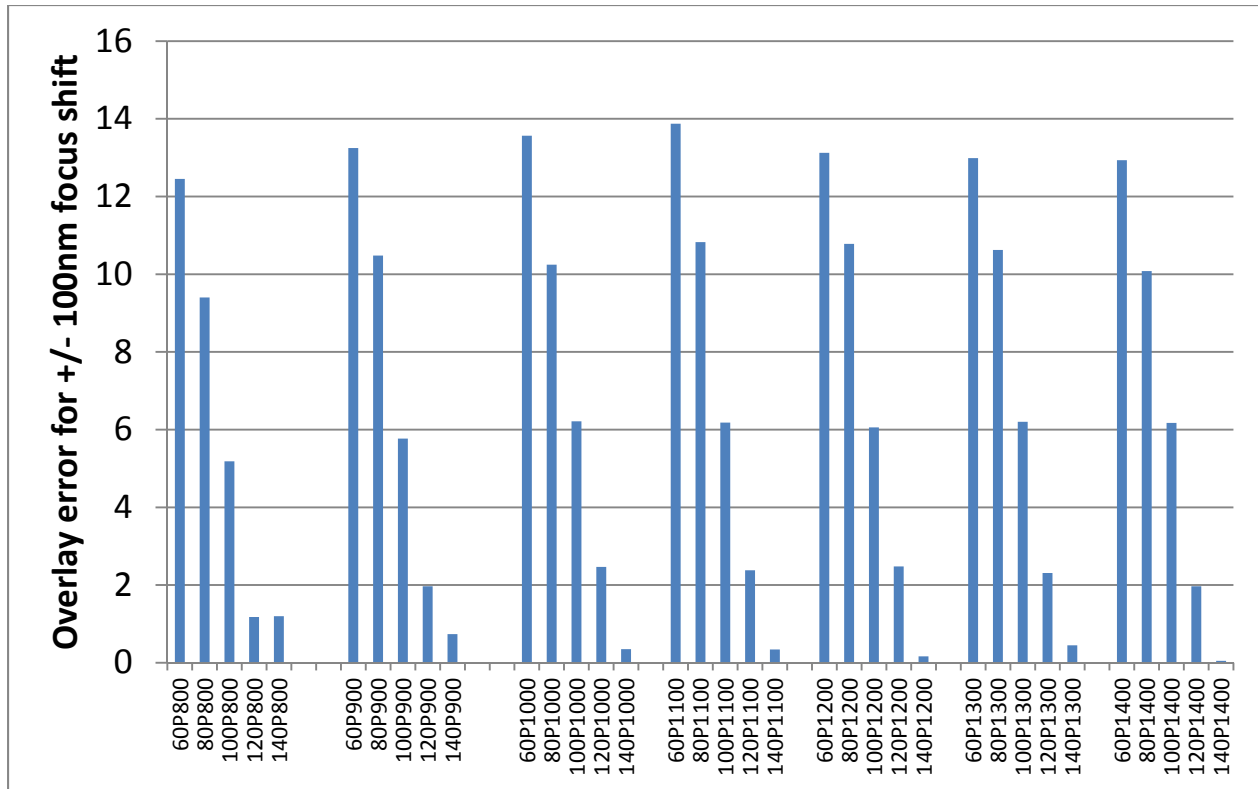
Fig. 10. Simulated total overlay error from +/- 100 nm defocus for various absorber CD and pitches.

4. CONCLUSION

A Phase Shift Mask (PSM) structure is proposed for use in focus monitoring. Both 90.9º and 180º phase shifts have been achieved. Both the EUV images of the focus monitor patterns on the new EUV PSM test mask, obtained from the SEMATECH/Berkeley Actinic Inspection Microscope (AIT), and the SEMATECH EUV Micro Exposure Tool (MET), shows that an Alt. PSM EUV mask can be effectively used for EUVL focus monitoring.

ACKNOWLEDGEMENTS

REFERENCES

[1] T. Adams, "Applications of latent image metrology in microlithography," Proc. SPIE, **1463**, 294 (1991).
[2] S. Stalnaker, P. Luehrmann, J. Waelpoel, C. Sager, P. Reynolds, "Focal plane determination for sub-half micron optical steppers," Microelectronic Engineering **21**, 33 (1993).
[3] J.W. Bossung, "Projection printing characterization," Proc. SPIE, **100**, 80-84 (1977)
[4] T. A. Brunner, A. L. Martin, R. M. Martino, C. P. Ausschnitt, T. H. Newman, M. S. Hibbs, "Quantitative stepper metrology using the focus monitor test mask," Proc. SPIE **2197**, 541 (1994).

[5] H. Nomura, "New phase shift gratings for measuring aberrations," Proc. SPIE **4346**, 25-35 (2001).

[6] B. L. Fontaine, M. V. Dusa, J. Krist, A. Acheta, J. Kye, H. J. Levinson, C. Luijten, C. B. Sager, J. J. Thomas, J. V. Praagh, "Analysis of Focus Errors in Lithography using Phase-Shift Monitors," Proc. SPIE **4691**, 315-324 (2002).

[7] M. McQuillan and B. Roberts, "Phase Shift Focus Monitoring Techniques," Proc. SPIE **6154**, 615430 (2006).

[8] O. Wood**,** J. Arnold**,** T. Brunner, etc. "Insertion strategy for EUV lithography," Proc. SPIE, **8322**, 832203 (2012).

[9] M. Sugawara, A. Chiba, H. Yamanashi and I. Nishiyama, "Alternating Phase Shift Mask in Extreme Ultra Violet Lithography," Jpn. J. Appl. Phys. **42**, 3776–3783 (2003)

[10] P. Y. Yan, "EUVL Alternating Phase Shift Mask Imaging Evaluation," Proc. SPIE **4889**, 1099-1105 (2002).

[11] P. Y. Yan, A. Myers, Y. Shroff, M. Chandhok, G. Zhang, E. Gullikson, and F. Salmassi, "EUVL Alternating Phase Shift Mask," Proc. SPIE **7969**, 79690G (2011).

[12] B. L. Fontaine, A. R. Pawloski, O. Wood, Y. Deng, H. J. Levinson, P. Naulleau, P. E. Denham, E. Gullikson, B. Hoef, C. Holfeld, C. Chovino, F. Letzkus, "Demonstration of Phase-Shift Masks for Extreme-Ultraviolet Lithography," Proc. SPIE **6151**, 61510A (2006).

[13] S. I. Han, E. Weisbrod, Q. Xie, P. J. S. Mangat, S. D. Hector, W. J. Dauksher, "Design and method of fabricating phase-shift masks for extreme-ultraviolet lithography by partial etching into the EUV multilayer mirror," Proc. SPIE **5037**, 314-330 (2003).

[14] C. Constancias, M. Richard, D. Joyeux, J. Chiaroni, R. Blanc, J. Y. Robic, E. Quesnel, V. Muffato, "Phase shift mask for EUV lithography," Proc. SPIE **6151**, 61511W (2006).

[15] G. Fenger, B. Smith, O. Wood, S. Raghunathan, L. Sun, T. Wallow, D. Civay, P. Mangat, H. Rolff, M. Bender, T. Schedel, I. Mochi, K. Goldberg, C. Anderson, P. Denham and E. Gullikson, "Aberration Metrology using Resist Images from a Strong Phase Shifting Mask," submitted to EIPBN (2013).

[16] J. W. Goodman, [Introduction to Fourier Optics], Roberts and Company Publishers, 3rd ed., (2004).

[17] T. A. Brunner, M. S. Hibbs, B. B. Peck and C. A. Spence, "Optical focus phase shift test pattern, monitoring system and process," US Patent 5,300,786 (1994)

[18] T. A. Brunner, C. P. Ausschnitt, "Method of improving grating test pattern for lithography monitoring and controlling," US Patent 7,455,939 (2008).